JOURNAL OF AGRICULTURAL AND FOOD CHEMISTRY

pubs.acs.org/JAFC Article

Ursolic Acid Alleviates DSS-Induced Colitis and Associated Liver Damage by Restoring Treg/Th17 Balance and Modulating Gut Microbiota and Its Histidine Metabolism

Man Zhao,[‖] Mengqi Liu,[‖] Fengyang Wu,[‖] Chong Li, Shudong Liu, Xinyu Yang, Zhonghua Wei, Baojiang Chen,* and Shuaijuan Han*

Cite This: https://doi.org/10.1021/acs.jafc.5c00220 Read Online

ACCESS | Metrics & More | Article Recommendations | Supporting Information

ABSTRACT: Ursolic acid (UA), a natural compound abundant in fruits and vegetables, exhibits established anti-inflammatory and hepatoprotective properties. This study investigated the therapeutic potential of UA as a dietary supplement for DSS-induced colitis and secondary liver injury using both an *in vivo* DSS-induced colitis mouse model and an *in vitro* intestinal epithelial cell model. Colitis model mice were administered UA at doses of 5, 25, 100, and 250 mg/kg. Through comprehensive analyses, including enzyme-linked immunosorbent assay (ELISA), immunohistochemistry (IHC), immunofluorescence (IF), Western blot, 16S rRNA sequencing, untargeted metabolomics, and transcriptomics, we demonstrated that 25 mg/kg UA optimally alleviated colitis symptoms. The mechanism involves restoring the balance between T regulatory cells (Treg) and T helper 17 cells (Th17) to reduce inflammation, potentially mediated by increased production of propionate from short-chain fatty acid (SCFA)-producing bacteria. Additionally, UA inhibits *Escherichia coli* (*E. coli*) growth through the action of the microbial metabolite L-histidine, thereby enhancing intestinal barrier integrity and inhibiting pyroptosis. Moreover, 25 mg/kg of UA exerts protective effects against liver injury by suppressing inflammation-related signaling pathways in colitis mice. These findings position UA as a promising functional food component for managing colitis and its hepatic complications.

KEYWORDS: *ursolic acid, colitis, Treg/Th17 balance, gut microbiota, secondary liver injury*

INTRODUCTION

Inflammatory bowel diseases (IBD), which encompass ulcerative colitis (UC) and Crohn's disease (CD), are marked by chronic and recurring intestinal inflammation.[1] IBD has a high incidence rate, leads to reduced quality of life, and is associated with the progression of colorectal cancer, posing a growing global public health challenge.[2]

Recent studies suggest that IBD arises from a complex interaction among environmental factors, immune-mediated responses, and microbial influences in genetically predisposed individuals,[3] manifested by immune response imbalance, abnormal cytokine production, barrier damage, and gut microbiota dysbiosis.[4,5] Th17 cells contribute to the pathology by producing proinflammatory cytokines as IBD progresses, while Treg cell activity, which can suppress Th17 activity, is reduced.[5,6] Restoring balance between Th17 and Treg cells could be an effective strategy for managing IBD. Gut microbiota imbalance is believed to actively drive inflammation in IBD rather than merely being a consequence of prolonged inflammatory responses.[7] Specifically, microbiota alterations can disrupt the Th17/Treg equilibrium in IBD, exacerbating inflammatory responses.[8,9] Conversely, certain probiotic bacterial strains directly modulate IBD progression.[10−12] Beyond microbial signaling, depletion of microbiota-derived metabolites is also a key research area in IBD, with notable examples being short-chain fatty acids (SCFAs), tryptophan, and bile acid metabolites.[3,5,7,13] Thus, restoring gut microbiota homeostasis and its metabolic output may represent a promising IBD treatment approach.

IBD can affect several organ systems, with secondary liver injury being the most prevalent extraintestinal manifestation in IBD patients.[1] Research indicates patients with IBD exhibit a 4-fold higher incidence of liver disease compared to the general population.[14] The underlying mechanisms of IBD-related liver injury may include leaky bowel syndrome and the presence of proinflammatory cytokines.[1,15] In particular, impaired gut integrity in the IBD permits the translocation of inflammatory mediators and toxins to the liver, potentially driving hepatic damage. This process ultimately induces liver injury by triggering immune cell activation and an inflammatory cascade. Furthermore, progressive liver dysfunction may exacerbate IBD severity, indicating a bidirectional relationship between liver and gut pathology.[16]

Beyond pharmacological treatment, dietary modification represents a viable therapeutic approach for IBD management.[9,17] Ursolic acid (UA), a pentacyclic triterpenoid carboxylic acid commonly present in various foods including

Received: January 6, 2025
Revised: June 9, 2025
Accepted: June 9, 2025

apples, rosemary, thyme, and hawthorn, has attracted significant interest due to its diverse biological activities.[18−20] UA exhibits multiple beneficial effects, including reducing inflammation, oxidative damage, and regulating gut microbiota, together providing a rampart against colitis.[21−23] Previous studies have demonstrated that UA can ameliorate inflammatory cell infiltration, thereby alleviating ulcerative colitis.[24] UA has been identified as the main active compound in both *Chaenomeles speciosa* leaves and *Fraxini Cortex* for alleviating colitis.[25,26] Furthermore, UA possesses notable hepatoprotective properties and therapeutic benefits for several liver conditions.[22,23,27] Despite its multifaceted biological activities, the exact molecular mechanism by which UA mitigates colitis and secondary liver injury remains unknown. Given these findings, this study sought to elucidate the therapeutic potential and mechanistic basis of dietary UA supplementation against experimental colitis and secondary liver injury, focusing on the regulation of pathways related to intestinal immune balance, microbial dysbiosis, intestinal barrier function impairment, pyroptosis, and liver inflammation was studied. Our results highlight the potential of UA as a functional food component for IBD management.

MATERIALS AND METHODS

Animals. Eight-week-old female C57BL/6J mice were maintained in an environment with a 12 h light-dark cycle at 22 °C. The mice were obtained from SPF Biotechnology Co., Ltd. (Beijing, China). All procedures were conducted in accordance with the ARRIVE guidelines and were approved by the Animal Experimentation Ethics Committee of Hebei Agricultural University (Protocol No. 2023058).

DSS-Induced Colitis and UA Treatment. Mice with chemically induced colitis were administered 3.0% (w/v) dextran sodium sulfate (DSS; 36−50 kDa; Catalog No. 02160110, MP Biomedicals, USA) sodium in water for 7 days. Following DSS treatment, UA (98%, Shenniu Pharmaceutical Co., Ltd., China) was administered orally at doses of 5, 25, 100, and 250 mg/kg/day from day 8 to day 21. The UA used in this study was extracted from rosemary. All mice received a vehicle consisting of 1% Tween 80 and 0.5% sodium carboxymethyl cellulose in equal volumes. UA was dissolved in the vehicle and administered via intragastric gavage. The experimental groups (n = 10/group) were as follows: the control group (CON), the DSS group (DSS), the DSS + 5 mg/kg UA group (DSS + UA 5), the DSS + 25 mg/kg UA group (DSS + UA 25), the DSS + 100 mg/kg UA group (DSS + UA 100), and the DSS + 250 mg/kg UA group (DSS + UA 250). The UA doses used in this study were rigorously determined based on preliminary research and our group's prior experiments.[18,28] Body weight and mortality were recorded daily. Colitis severity was evaluated using the disease activity index (DAI).[5] During the experimental period, a total of 10 animals died, with the percent survival distribution across groups presented in Figure S1. At the end of the experiment, six mice per group were euthanized. Blood samples were collected post-anesthesia, centrifuged at 4 °C for 3500g, and the serum was separated. Colon length was measured upon sacrifice. Colon tissues were fixed in 4% paraformaldehyde for histological analysis. Mouse feces, colon, and liver tissues were collected aseptically, and samples were preserved at −80 °C after flash freezing in liquid nitrogen.

Histopathology. Colon and liver specimens were fixed, paraffin-embedded, and sectioned for hematoxylin-eosin (H&E) staining. A qualified pathologist evaluated the colon sections.[4] The detailed material is given in Supporting Information S1.

Enzyme-Linked Immunosorbent Assay (ELISA) and Serum Biochemical Indicators. The concentrations of cytokines, including interleukin (IL)-1β, tumor necrosis factor (TNF)-α, IL-6, IL-10, IL-17A, transforming growth factor (TGF)-β, and lipopolysaccharide (LPS) were quantified using ELISA kits (Jiangsu Meimian Industrial Co., Ltd., Yancheng, China). The serum levels of aspartate transaminase (AST) and alanine aminotransferase (ALT) were determined using the corresponding biochemical assay kits (Nanjing Jiancheng Bioengineering Institute, Nanjing, China).

Quantitative Reverse Transcription-Polymerase Chain Reaction (qRT-PCR). The detailed material is given in Supporting Information S2. The expression levels of target genes and β-*actin* mRNA were normalized based on the cycle threshold (CT) values. The relative expression of target genes was calculated by using the $2^{-\Delta\Delta CT}$ method. Primer information is provided in Table S1.

Immunohistochemistry (IHC). The detailed material is given in Supporting Information S3.

Immunofluorescence (IF). The detailed material is given in Supporting Information S4.

16S rRNA. Microbial DNA was isolated utilizing the EZNA Soil DNA Kit (Omega Biotek, GA, USA). Primer pairs 338F (5′-ACTCCTACGGGAGGCAGCAG-3′) and 806R (5′-GGACTACHVGGGTWTCTAAT-3′) were employed to amplify the V3−V4 hypervariable region of the bacterial 16S rRNA gene. The PCR products were combined equally, purified, and subsequently sequenced on an Illumina platform (PE300, Illumina, San Diego, USA). To assess microbial community similarity, Principal Coordinate Analysis (PCoA) and Adonis testing were conducted by using the "Vegan" package. The gut microbial health index (GMHI)[29] and the microbial dysbiosis index (MDI)[30] were calculated to assess the health status and dysregulation of the gut microbiome, respectively. The differential abundance of bacterial taxa was determined by using the Kruskal−Wallis test, and the Linear Discriminant Analysis Effect Size (LEfSe) method was applied to identify significantly enriched bacterial taxa across the different groups.

Determination of SCFAs. The detailed material is given in Supporting Information S5. The SCFA content in the extracted solution was analyzed using the gas chromatograph.

Bacterial Translocation. The detailed material is given in Supporting Information S6. Primer sequences for *E. coli* are shown in Table S1.

Liquid Chromatography−Mass Spectrometry Analysis (LC-MS Analysis). Samples underwent metabolite extraction with a methanol−water mixture. Metabolite analysis was performed using a SCIEX UPLC-Triple TOF 6600 system. Raw data for peak detection and alignment were processed with Progenesis QI 2.3 software. Metabolites present in at least 80% of the samples were retained, and log10 transformed data were used. Partial least-squares discriminant analysis (PLS-DA) was conducted using the "ropls" package (version 1.6.2). Metabolites with a variable importance projection (VIP) > 1 and $p < 0.05$ were identified as differential metabolites. Pathway enrichment analysis of differential metabolites was performed using the KEGG database. The Receiver Operating Characteristic (ROC) curve was applied to validate the predictive accuracy of the results.

Determination of L-Histidine. Fecal L-histidine was quantified by LC-MS with precolumn derivatization using 6-aminoquinolyl-*N*-hydroxysuccinimidyl carbamate. Initially, the analytes underwent deproteinization using a 5% trichloroacetic acid solution. Following this, the samples were centrifugated (12,000 rpm, 4 °C, 10 min). The concentrations of hesitodine were then determined in each sample.

Cell Culture and *E. coli* Infection. Human colonic epithelial cell line Caco-2 (Pricella, Wuhan, China) was maintained in DMEM supplemented with 10% fetal bovine serum. Cells (density: 5×10^4 cells/cm^2) were cultured in 96-well plates and treated with various levels of L-Histidine (0, 1, 5, 10, and 20 ng/mL; Sigma-Aldrich, PA, USA) for 12 h. CCK-8 was added, and the mixture was incubated for 2 h. A 10-fold coculture of *Escherichia coli* (*E. coli* O157:H7 strain, ATCC35150, China) was performed for 2 h. The cell supernatant was collected for measuring the levels of IL-1β and TNF-α.

Western Blot Assay. The detailed material is given in Supporting Information S7. Information on the antibodies used is provided in Table S2.

RNA Sequencing and Analysis. RNA-seq libraries were prepared using the Illumina Stranded mRNA Prep Kit (San Diego, CA, USA). After size selection (300 bp) and PCR amplification, libraries were quantified (Qubit 4.0) and sequenced (NovaSeq 6000; 2 × 150 bp). Raw reads were quality-filtered (Fastp) and aligned to the GRCh38

https://doi.org/10.1021/acs.jafc.5c00220
J. Agric. Food Chem. XXXX, XXX, XXX−XXX

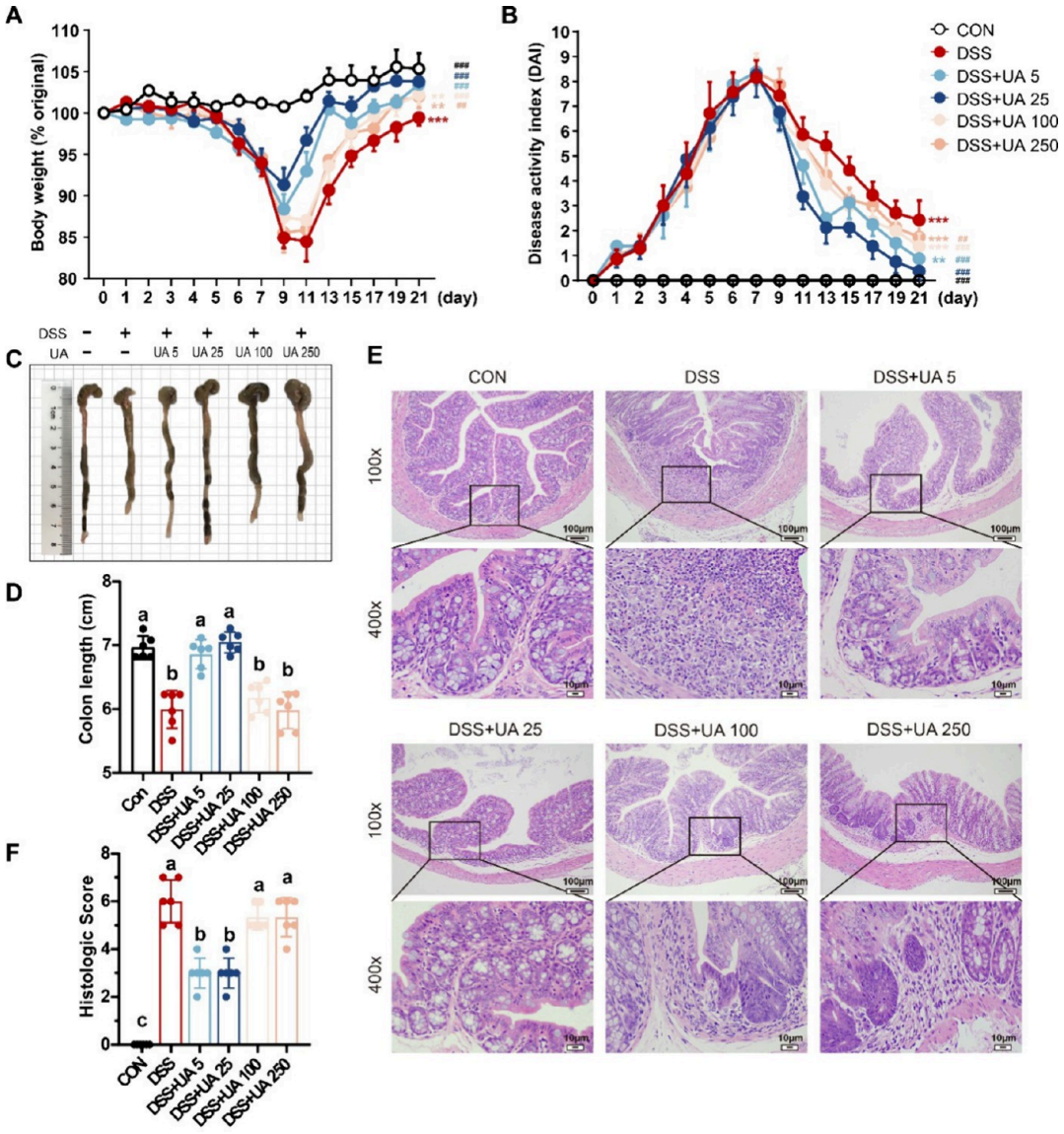

Figure 1. UA intake ameliorated DSS-induced colitis. (A) Body weight change. (B) DAI score. Compared with the CON group; #: Compared to the DSS group). (C,D) Colon length. (E) Representative microscopic pictures of H&E staining (100× and 400× magnification). (F) Histology score. ** $p < 0.01$, *** $p < 0.001$. ## $p < 0.01$, ### $p < 0.001$. $n = 6$.

reference genome (HISAT2). Gene expression was quantified as TPM using RSEM. Differential expression analysis (DESeq2) identified genes with $|\log2FC| \geq 1$ and FDR < 0.05 as significant.

Weighted Gene Correlation Network Analysis (WGCNA). WGCNA was performed on liver transcriptome data using the "WGCNA" package.[21,31] To determine the optimal soft-threshold parameter, the pickSoftThreshold function was utilized, yielding a value of $\beta = 8$. A minimum of 30 mRNAs per module was set as a threshold, while other parameters remained at their default values to aid in module identification and network construction. KEGG pathway enrichment analysis for genes within the modules was performed using KOBAS. The target genes linked to these key mRNAs were screened and identified, leading to the construction and visualization of a regulatory network map for the mRNAs using Cytoscape (Version 3.9.0).

Statistical Analysis. The data were analyzed using one-way analysis of variance (ANOVA) by the Statistical Package for the Social Sciences (SPSS) version 26. Differences between means were assessed using Tukey's multiple range test. Results are reported as the mean ± standard deviation (SD), with significance defined as $p < 0.05$.

RESULTS

UA Intake Ameliorated DSS-Induced Experimental Colitis. Compared to the DSS group, the DSS + UA 5 and DSS + UA 25 groups exhibited significantly improved outcomes, including reduced mortality (Figure S1), decreased weight loss (Figure 1A), lower DAI scores (Figure 1B), and increased colon length ($p < 0.05$) (Figure 1C,D). Relative to the DSS group, the DSS + UA 5 and DSS + UA 25 groups showed significantly less crypt deformation and fewer inflammatory cell infiltrates ($p < 0.05$) (Figure 1E,F).

UA Intake Reduced Inflammation Intensity and Th17/Treg Imbalance in Colitis Mice. In the DSS + UA 25 group, the concentrations of IL-1β, TNF-α, IL-6, and IL-17A in both the colon and serum were notably lower than those in the DSS group ($p < 0.05$) (Figure 2A–L). Moreover, the serum and colon levels of TGF-β and IL-10 were notably higher in the DSS + UA 25 group ($p < 0.05$) (Figure 2A–L). These results collectively suggest that UA can effectively alleviate inflammation in this IBD model, with the DSS + UA 25 group exhibiting a

https://doi.org/10.1021/acs.jafc.5c00220
J. Agric. Food Chem. XXXX, XXX, XXX−XXX

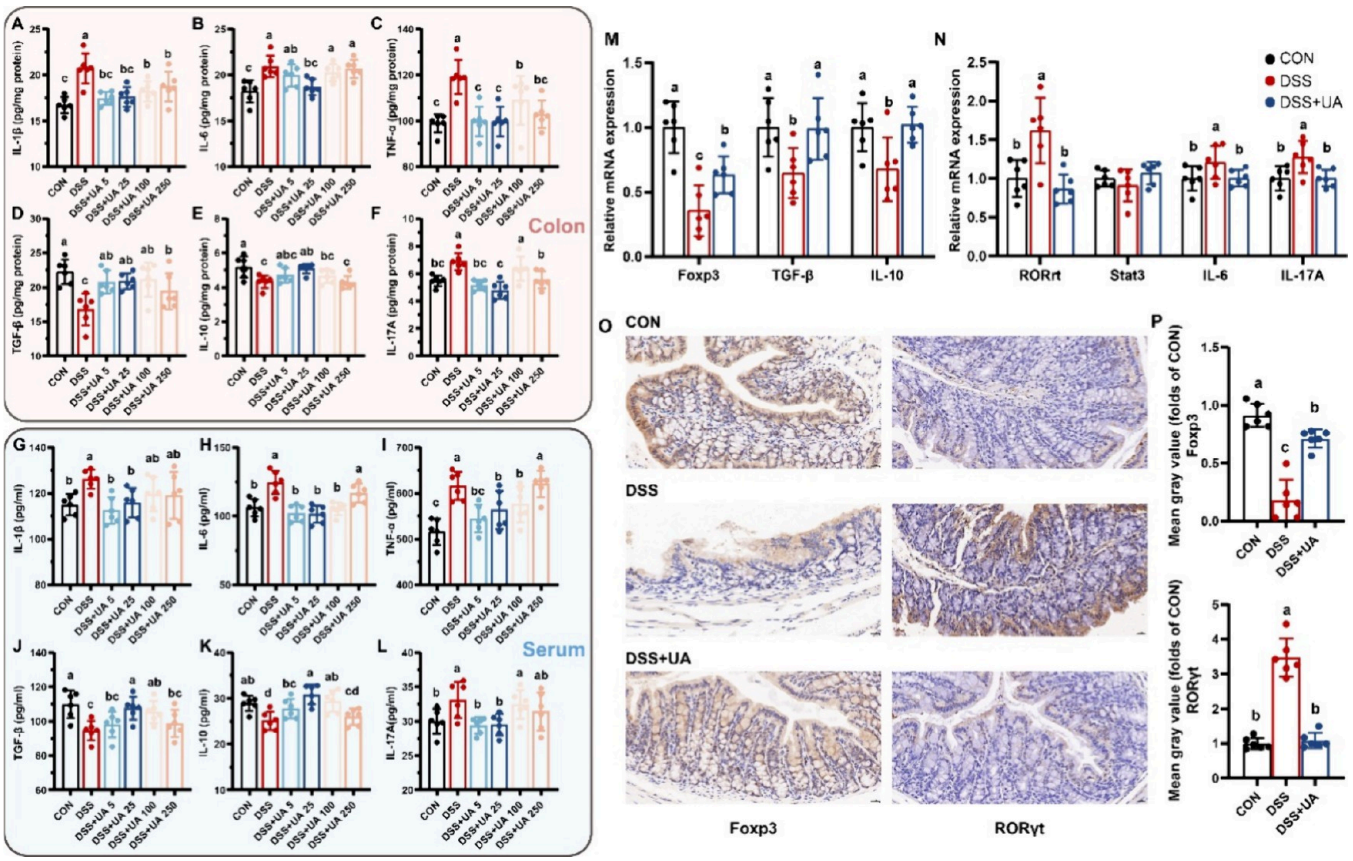

Figure 2. UA intake reduced inflammation intensity and Th17/Treg imbalance in colitis mice. (A) IL-1*β*, (B) IL-6, (C) TNF-*α*, (D) TGF-*β*, (E) IL-10, and (F) IL-17A cytokine levels in colon tissue homogenate. (G) IL-1*β*, (H) IL-6, (I) TNF-*α*, (J) TGF-*β*, (K) IL-10, and (L) IL-17A cytokine levels in serum. (M) The relative mRNA expression of Treg differentiation-related genes. (N) The relative mRNA expression of Th17 differentiation-related genes. The protein expression levels of (O) Foxp3 and RORγt (immunohistochemical staining) and (P) statistical analysis. $n = 6$.

superior therapeutic effect compared to the other groups. Therefore, this group (subsequently called the DSS + UA group) was selected for mechanism exploration. Given the critical role of the Treg/Th17 balance in regulating inflammatory cytokine secretion, we investigated UA's influence on this balance. Relative to DSS controls, the DSS + UA group exhibited a notable rise in mRNA expression for Treg differentiation markers (forkhead box p3 (*Foxp3*), *TGF-β*, and *IL-10*) ($p < 0.05$) (Figure 2M), as well as a decrease in the mRNA levels of Th17 differentiation markers (retinoic acid-related orphan receptor gamma t (*RORγt*), *IL-6*, and *IL-17A*) ($p < 0.05$) (Figure 2N). Additionally, compared with the DSS group, Foxp3 protein expression in the DSS + UA group was significantly elevated, while RORγt protein expression was markedly decreased ($p < 0.05$) (Figure 2O−P, Figure S2).

UA Intake Induced Significant Alterations in the Gut Microbiota of Colitic Mice. The rarefaction curves, Shannon curves, and rank abundance curves from the sequencing analysis are presented in Figure S3(A−C). No significant differences in the Shannon index were detected among the three groups ($p > 0.05$) (Figure S3D). The PCoA and Adonis analysis revealed significant differences in microbiota structure among the groups ($p < 0.05$) (Figure 3A−C). The DSS challenge significantly decreased the GMHI index while increasing the MDI index, both of which were notably improved following UA intake ($p < 0.05$) (Figure 3D−G).

Figure S3(E,F) shows the 10 most abundant phyla and the top 15 genera present. The taxonomic markers across the groups were screened by LEfSe (LDA ≥ 2, $p < 0.05$) (Figure 3H), and differential genera were further identified by the Kruskal−Wallis H test among the three groups ($p < 0.05$) (Figure 3I). The differential bacteria including *Odoribacter*, *Alistipes*, *Turicibacter*, *Staphylococcus*, *Achromobacter*, *Escherichia-Shigella*, *Solibacillus*, *Paenalcaligenes*, *Paludicola*, and *Psychrobacter* were identified as taxonomic markers in the DSS group, and *Dubosiella*, *Parasutterella*, *Clostridium_sensu_stricto_1*, *Christensenellaceae_R-7_group*, *Bilophila*, and *Aerococcus* were identified as taxonomic markers in the DSS + UA group. Importantly, UA treatment significantly reversed the increase in relative abundance of the harmful bacteria *Escherichia-Shigella* (genus level; Figure S4) and *Escherichia coli* (species level; Figure S5) induced by the DSS challenge ($p < 0.05$). Additionally, UA significantly mitigated the decrease in propionic acid levels induced by DSS challenge ($p < 0.05$) (Figure 3J).

UA Inhibits *E. coli* Proliferation and LPS Production to Protect the Intestinal Barrier and Alleviate DSS-Induced Colitis. The UA intake group showed a notable decrease in *E. coli* levels in fecal samples ($p < 0.05$) (Figure 4A). Although the DSS challenge decreased the counts of *E. coli* in both colon and liver tissues, UA intake notably lowered *E. coli* counts in these organs ($p < 0.05$) (Figure 4B−D). Additionally, various genes involved in LPS synthesis were markedly enriched in the DSS group, while UA intake effectively diminished the prevalence of these genes ($p < 0.05$) (Figure 4E). We also examined LPS concentrations in the colon and blood and found consistent significant changes ($p < 0.05$) (Figure 4F,G). Our results

https://doi.org/10.1021/acs.jafc.5c00220
J. Agric. Food Chem. XXXX, XXX, XXX−XXX

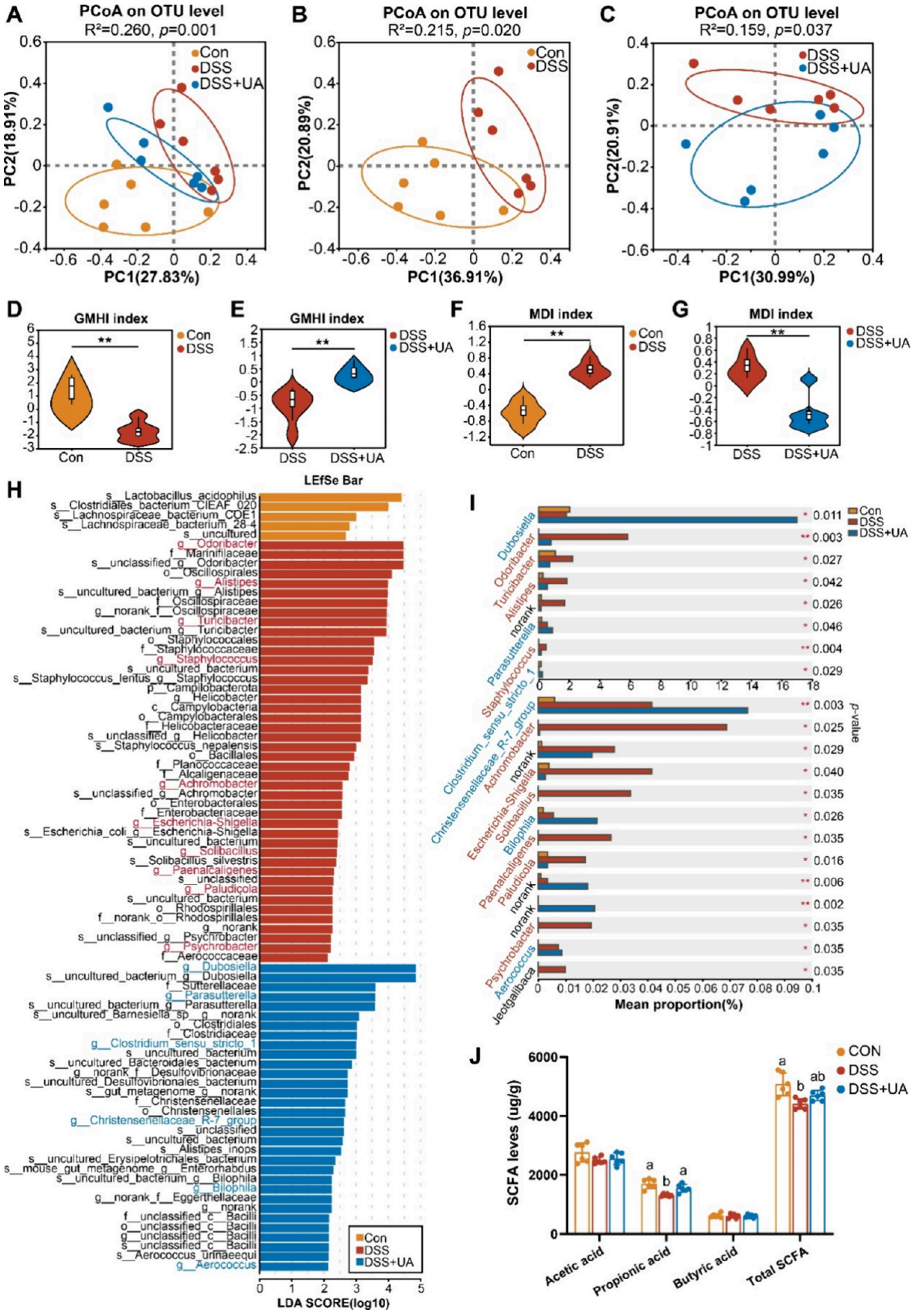

Figure 3. UA intake significantly altered the gut microbiota in colitis mice. (A−C) Principal coordinate analysis (PCoA). (D,E) Gut microbial health index (GMHI). (F,G) Microbial dysbiosis index (MDI). (H) LEfSe identified the marker bacteria in each group (LDA ≥ 2). (I) Different bacteria at the genus level. (J) The short-chain fatty acid levels. * $p < 0.05$, ** $p < 0.01$. $n = 6$.

https://doi.org/10.1021/acs.jafc.5c00220
J. Agric. Food Chem. XXXX, XXX, XXX−XXX

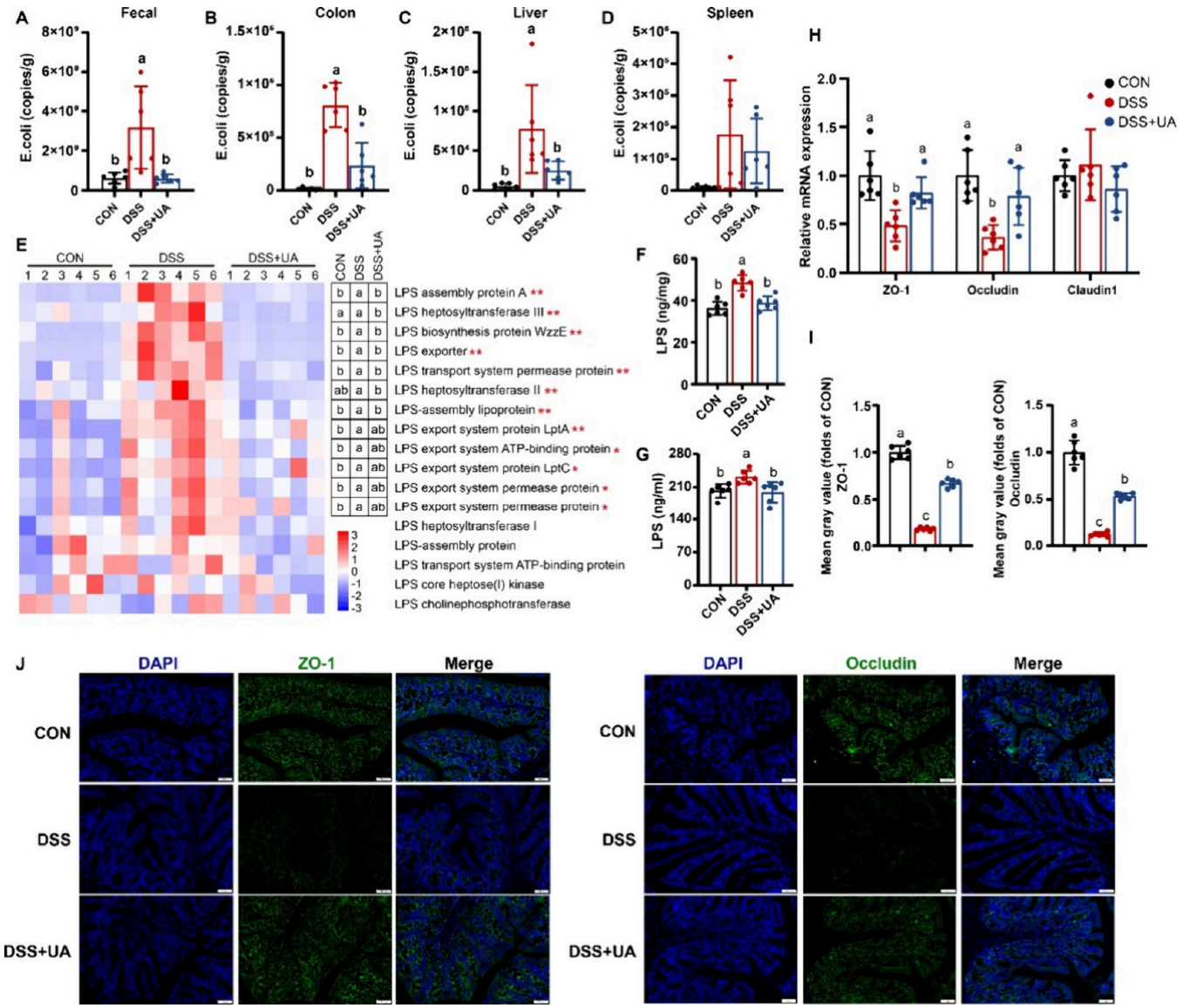

Figure 4. UA reduces bacterial translocation and LPS levels and protects against intestinal barrier damage in colitis mice. qRT-PCR analysis of pathogenic *E. coli* detected in the (A) fecal, (B) colon, (C) liver, and (D) spleen. (E) Predicted PICRUST2 bacterial community function. Effect of UA on LPS in (F) colon and (G) serum in mice colitis. (H) The relative mRNA expression of tight-junction-related genes. (I) The relative protein expression levels of ZO-1 and Occludin (immunohistochemical staining) and (J) statistical analysis. * $p < 0.05$, ** $p < 0.01$. $n = 6$.

demonstrated that the mRNA and protein expressions of ZO-1 and occludin in the DSS + UA group significantly higher compared with the DSS group ($p < 0.05$) (Figure 4H–J).

Correlation analysis revealed a strong positive association between LPS levels and *E. coli* counts ($p < 0.05$) (Figure 5A–D). Furthermore, colonic LPS levels showed a positive correlation with IL-1β, TNF-α, IL-17A, and histological scores ($p < 0.05$). We noted significant positive correlations between fecal *E. coli* and colonic IL-1β, TNF-α, and IL-17A ($p < 0.05$). The abundance of *E. coli* exhibited a positive association with histological scores but an inverse relationship with ZO-1 and occludin expression ($p < 0.05$) (Figure 5E). To assess pyroptosis levels, we found that the mRNA expression levels of toll-like receptor 4 (*TLR4*), NOD-like receptor family pyrin domain containing 3 (*NLRP3*), cysteinyl aspartate specific proteinase 1 (*Caspase 1*), and gasdermin D (*GSDMD*) were significantly lower in the DSS + UA group compared to the DSS group ($p < 0.05$) (Figure 5F).

UA Significantly Modifies the Metabolite Profile in Colitis Mice. The PLS-DA model revealed significant separation of metabolic profiles between the DSS and CON groups (Figure 6A) and between the DSS and DSS + UA groups (Figure 6B). Compared with the DSS group, administration of UA led to marked changes in 66 metabolite concentrations (VIP > 1, $p < 0.05$) (Figure 6C).

Numerous differential metabolites were enriched in several metabolic pathways (FDR < 0.05), including histidine metabolism, aminoacyl-tRNA biosynthesis, bisphenol degradation, and linoleic acid metabolism (Figure 6D). Given the significant impact on histidine metabolism, we constructed histidine-related metabolic pathways based on the KEGG database (Figure 6E). The findings revealed that L-histidine was significantly enriched in the DSS + UA group, while its degradation product, formiminoglutamic acid, was markedly decreased, and levels of L-asparagine increased significantly ($p < 0.05$). Additionally, ROC curve analysis indicated that L-

https://doi.org/10.1021/acs.jafc.5c00220
J. Agric. Food Chem. XXXX, XXX, XXX−XXX

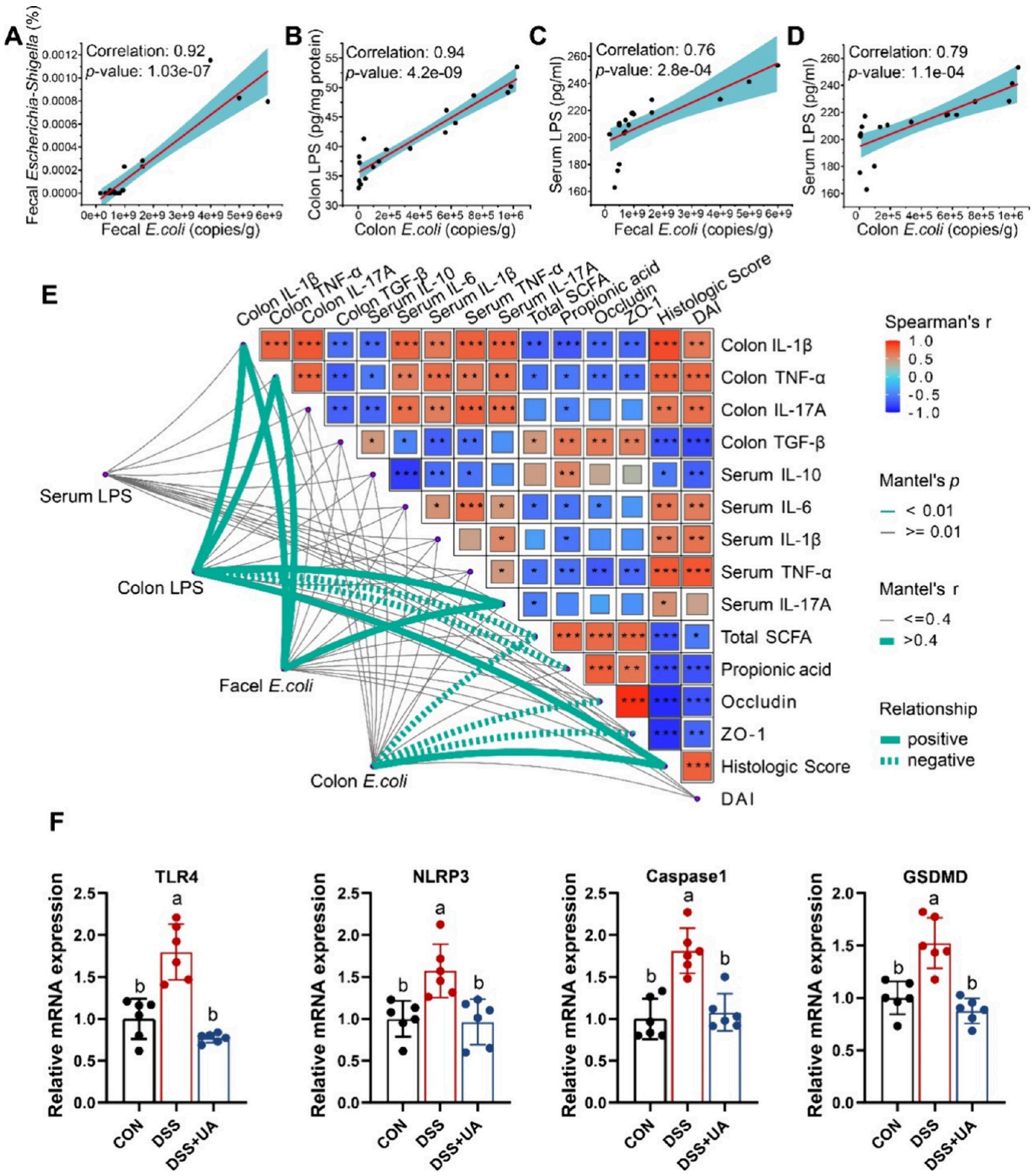

Figure 5. UA alleviated colitis by inhibiting the proliferation of *E. coli* and its LPS production. (A) Spearman correlation of fecal *E. coli* with fecal *Escherichia-Shigella*. (B) Spearman correlation of colon *E. coli* with colon LPS levels. (C) Spearman correlation of fecal *E. coli* with serum LPS levels. (D) Spearman correlation of colon *E. coli* with serum LPS levels. (E) Correlation between serum LPS, colon LPS, fecal *E. coli*, and colon *E. coli* and the above statistically significant indicators. (F) The relative mRNA expressions of *TLR4*, *NLRP3*, *Caspase 1*, and *GSDMD*. * $p < 0.05$, ** $p < 0.01$, *** $p < 0.001$. $n = 6$.

histidine had a high predictive value and could be used as a potential biomarker for UA to alleviate DSS-induced colitis (AUC = 0.917) (Figure 6F). We further validated these results by quantifying L-histidine in mouse feces, which confirmed the nontargeted metabolomics data ($p < 0.05$) (Figure 6G). Correlation analysis revealed a significant negative relationship between L-histidine and *Escherichia-Shigella* ($p < 0.001$) (Figure S6). Moreover, L-histidine concentration was negatively

https://doi.org/10.1021/acs.jafc.5c00220
J. Agric. Food Chem. XXXX, XXX, XXX−XXX

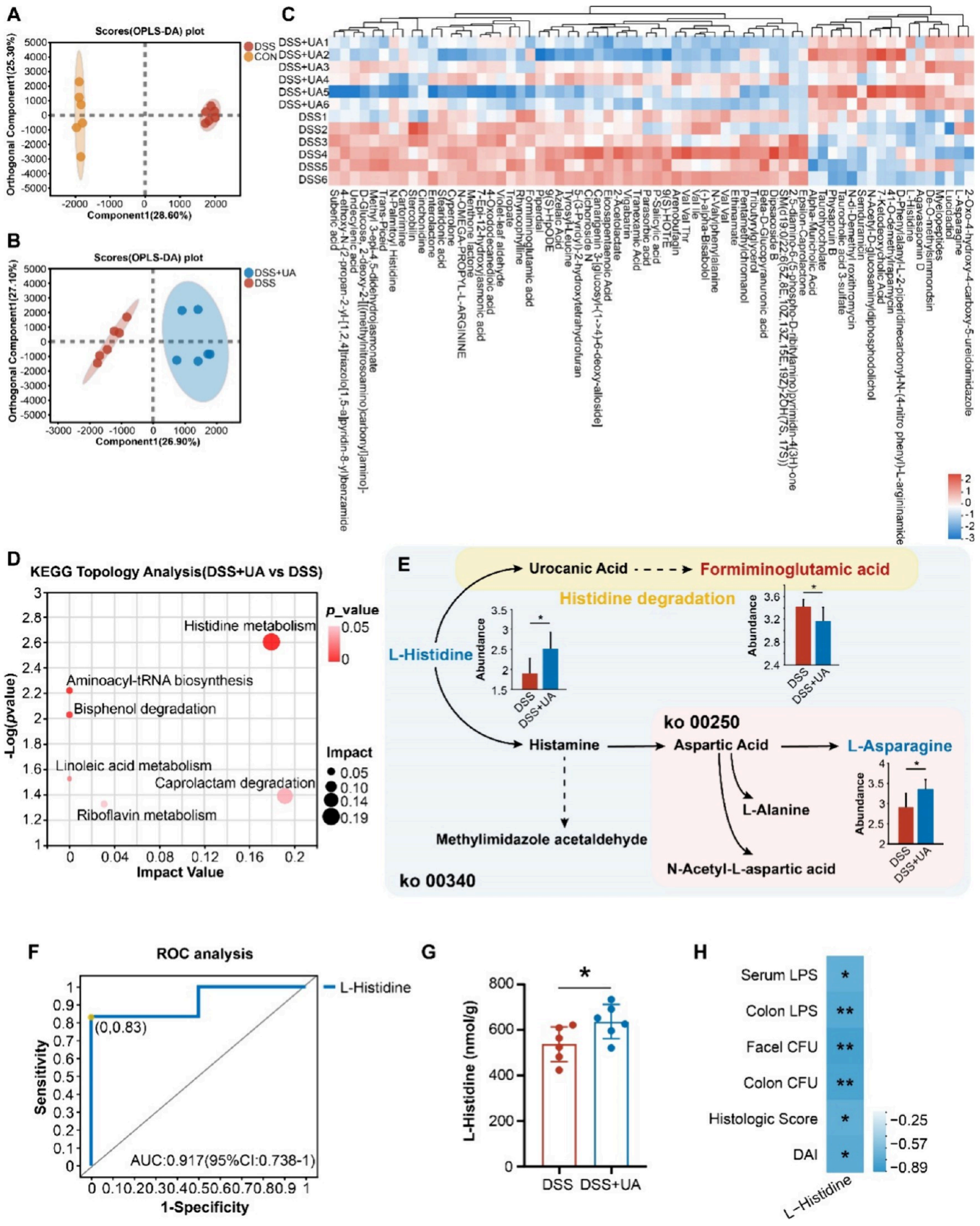

Figure 6. UA markedly alters the metabolite profile in colitis mice. (A,B) Partial Least Squares Discrimination Analysis (PLS-DA). (C) Heatmap of 66 different metabolites. (D) KEGG pathway enrichment analysis. (E) Histidine-related metabolic pathways. ko 00340, histidine metabolism; ko 00250, alanine, aspartate, and glutamate metabolism. (F) Receiver operating characteristic (ROC) curve. (G) Comparison of L-histidine content in fecal of colitis mice treated with UA. (H) Correlation analysis of L-histidine with LPS, *E. coli* copies number, histologic score, and DAI. * $p < 0.05$, ** $p < 0.01$. $n = 6$.

https://doi.org/10.1021/acs.jafc.5c00220
J. Agric. Food Chem. XXXX, XXX, XXX−XXX

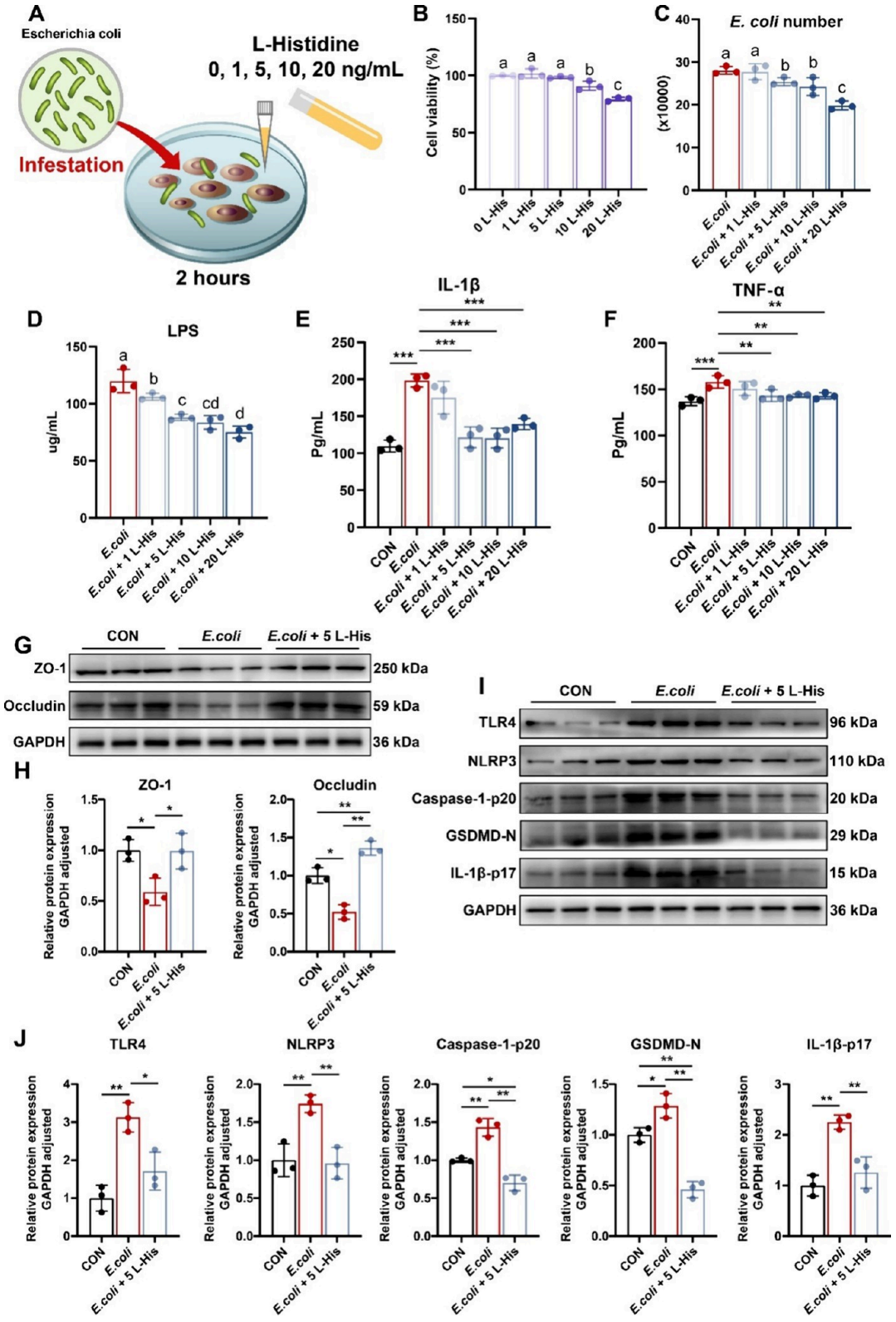

Figure 7. Protective effect of L-histidine against *E. coli* infection in vitro. (A) Schematic diagram. (B) Effect of different levels of L-histidine on cell viability. (C) *E. coli* proliferation number. (D) LPS levels. (E) IL-1β levels. (F) TNF-α levels. (G,H) The relative protein expression of ZO-1 and Occludin. (I,J) The relative protein expressions of TLR4, NLRP3, GSDMD-N, caspase-1-p20, and IL-1β-p17. * $p < 0.05$, ** $p < 0.01$, *** $p < 0.001$. $n = 3$.

correlated with LPS, *E. coli* copy number, histological scores, and DAI ($p < 0.05$) (Figure 6H).

L-Histidine Alleviated *E. coli*-Induced Inflammation, Tight Junction Disruption, and Pyroptosis in Colonic Epithelial Cells. We examined the effects of various

https://doi.org/10.1021/acs.jafc.5c00220
J. Agric. Food Chem. XXXX, XXX, XXX−XXX

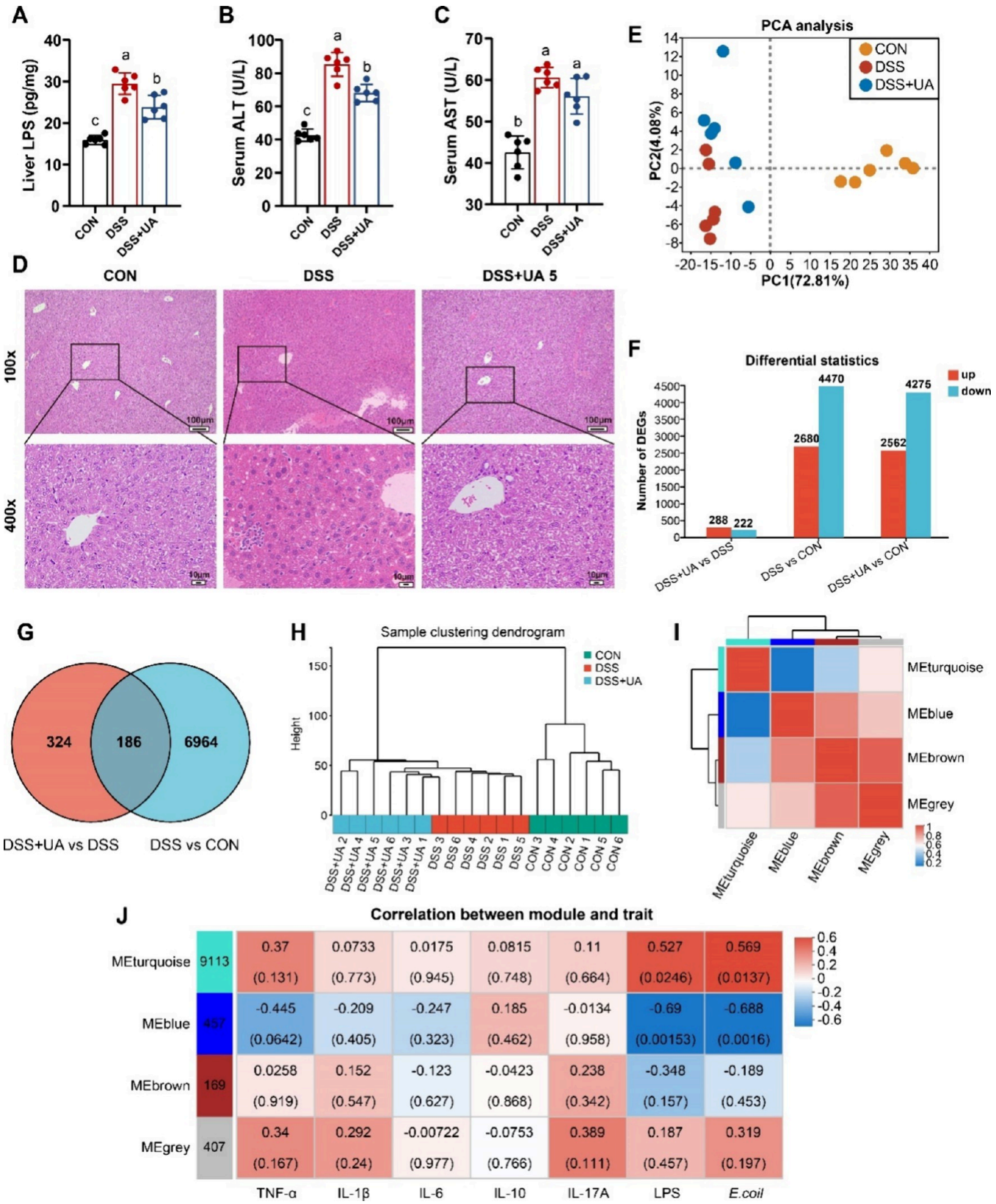

Figure 8. UA alleviates liver damage and changes liver transcriptional profile in colitis mice. (A) Level of LPS in the liver. (B,C) The levels of ALT and AST in serum. (D) Representative microscopic pictures of H&E staining (100× and 400× magnification). (E) PCA analysis of liver transcriptional profile. (F) The number of differential expression genes (DEGs) in each group was summarized. (G) Venn diagram. (H) Sample clustering dendrogram. (I) Correlation between modules. (J) Visualization of module-trait associations using a heatmap plot. $n = 6$.

concentrations of L-histidine on the inflammatory response to *E. coli* infection (Figure 7A). Our findings indicated that L-histidine concentrations below 5 ng/mL were not cytotoxic to the cells (Figure 7B). At concentrations of 5, 10, and 20 ng/mL, L-

https://doi.org/10.1021/acs.jafc.5c00220
J. Agric. Food Chem. XXXX, XXX, XXX−XXX

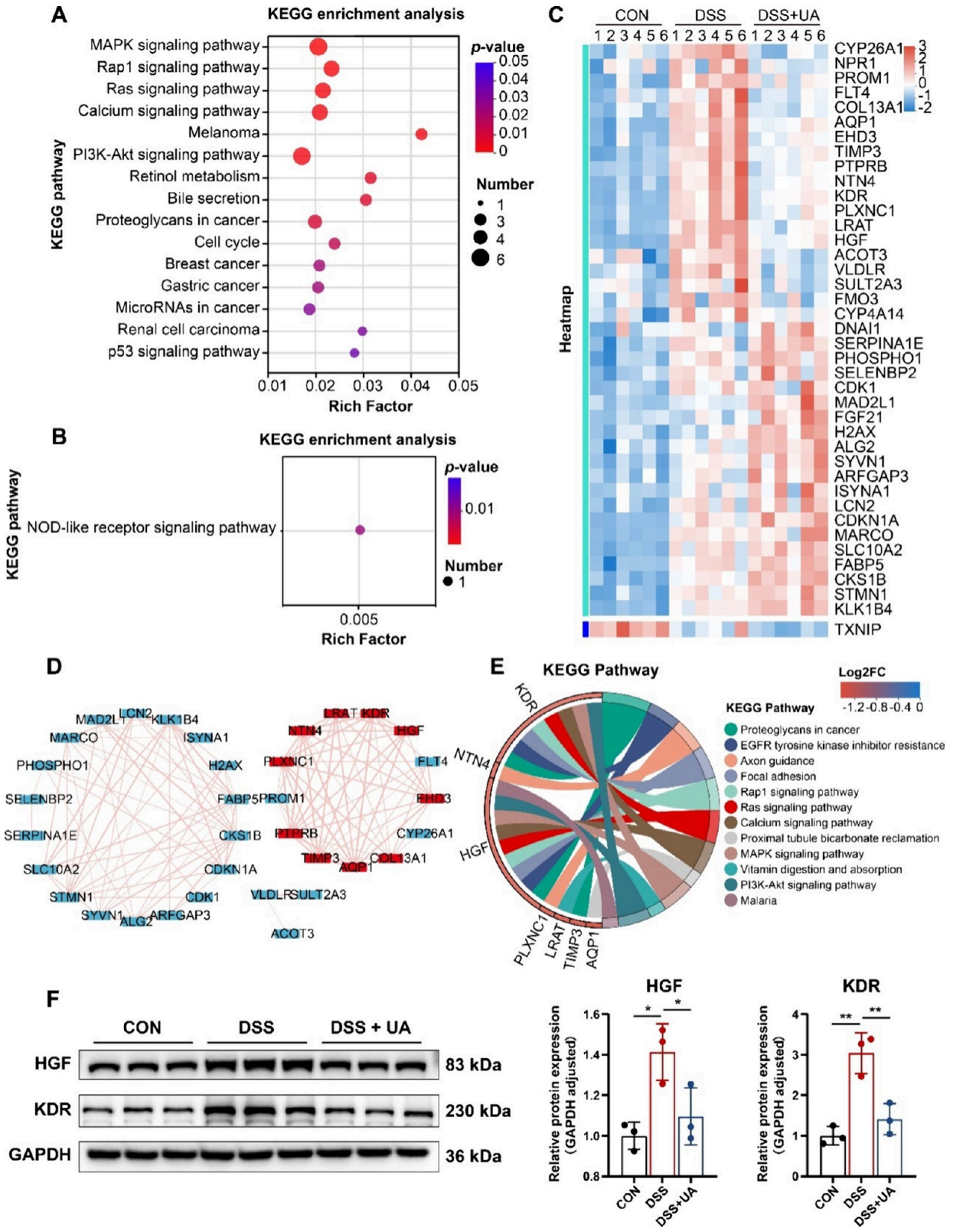

Figure 9. WGCNA analysis screened the key candidate genes of UA in alleviating liver injury in colitis mice. (A) KEGG pathway enrichment analysis (turquoise module). (B) KEGG pathway enrichment analysis (blue module). (C) DEGs participating in the KEGG pathway (turquoise and blue modules). (D) Correlation network diagram between DEGs ($|R| > 0.8$, $p < 0.05$). (E) KEGG pathway enrichment chord plot. $n = 6$. (F) The relative protein expression of HGF and KDR. * $p < 0.05$, ** $p < 0.01$. $n = 3$.

histidine significantly inhibited *E. coli* proliferation ($p < 0.05$) (Figure 7C), while LPS levels were significantly decreased at concentrations of 1, 5, 10, and 20 ng/mL ($p < 0.05$) (Figure 7D). Moreover, L-histidine at 5, 10, and 20 ng/mL notably lowered the levels of IL-1β and TNF-α ($p < 0.05$) (Figure 7E,F).

https://doi.org/10.1021/acs.jafc.5c00220
J. Agric. Food Chem. XXXX, XXX, XXX−XXX

We selected the *E. coli* + 5 ng/mL L-His group for further analysis because this concentration was nontoxic to cells while significantly reducing inflammatory factor levels. Our subsequent findings revealed that *E. coli* infection significantly decreased the expression of ZO-1 and occludin proteins in colonic epithelial cells, and this reduction was significantly reversed by L-histidine treatment ($p < 0.05$) (Figure 7G,H). Moreover, compared with the control group, the *E. coli* group exhibited significantly higher protein levels of TLR4, NLRP3, GSDMD-N, caspase-1-p20, and IL-1β-p17, all of which were significantly reduced following L-Histidine treatment ($p < 0.05$) (Figure 7I,J).

UA Alleviates Liver Injury in Colitis Mice. The DSS + UA group had significantly lower LPS content than the DSS group ($p < 0.05$) (Figure 8A). Moreover, UA administration led to a significant reduction in ALT concentrations ($p < 0.05$), while AST levels remained unchanged ($p > 0.05$) (Figure 8B,C). Histological analysis of HE staining revealed hepatic injury in DSS-treated mice, characterized by hepatocellular degeneration, cytoplasmic vacuolation, or fine lipid droplets, along with focal necrosis and inflammatory cell infiltration. UA administration markedly mitigated these histopathological alterations (Figure 8D). To investigate how UA exerts its hepatoprotective effects, we conducted liver tissue transcriptome profiling. Analysis identified 194 uniquely expressed genes in the CON group, 372 in the DSS group, and 189 in the DSS + UA group (Figure S7A). PCA demonstrated distinct transcriptomic characteristics across the three groups (Figure 8E, Figure S7B,C). We identified that a total of 510 DEGs were found in the DSS + UA group compared to the DSS group. Between the DSS and CON groups, we detected 7,150 DEGs, while 6,837 DEGs were identified between the DSS + UA and CON groups (Figure 8F). Additionally, a comparison between DSS + UA vs DSS and DSS vs CON revealed 186 DEGs (Figure 8G). We further validated the expression of 10 randomly selected mRNAs using qRT-PCR, demonstrating high concordance between sequencing and PCR data (correlation value = 0.885, $p < 0.01$) (Figure S8K).

We subsequently performed WGCNA on the transcriptome data, and no abnormal samples were detected in the hierarchical clustering analysis (Figure 8H). Highly correlated gene modules were identified, showing associations with LPS, *E. coli*, and various inflammatory factors (Figure S9A). WGCNA classified the transcriptome data into four modules, with the turquoise and blue modules showing significant correlations with both LPS and *E. coli* abundance ($p < 0.05$, $|r| > 0.5$) (Figure 8I,J). Scatter plots demonstrated a significant relationship between gene significance (GS) and module membership (MM), indicating that the genes within the turquoise and blue modules are strongly associated with LPS and *E. coli* counts (Figure S9B−E).

We then performed KEGG enrichment analysis on the DEGs in the blue and turquoise modules. The turquoise module showed significant enrichment in 15 KEGG pathways ($p < 0.05$), with the top three pathways being the MAPK signaling, Rap1 signaling, and Ras signaling pathways (Figure 9A). The blue module was significantly enriched in the NOD-like receptor signaling pathway ($p < 0.05$) (Figure 9B). Figure 9C shows the differential genes enriched in the KEGG pathways. Using the STRING database, we constructed a gene interaction network for the DEGs involved in KEGG pathways within the turquoise module, identifying 10 hub genes (Figure 9D). Finally, functional enrichment analysis of these hub genes indicated that *HGF* and *KDR* are involved in regulating multiple biological functions (Figure 9E). In comparison to the controls, DSS-treated mice exhibited markedly elevated HGF and KDR protein levels. However, UA treatment substantially reduced their expression ($p < 0.05$; Figure 9F).

DISCUSSION

UA is recognized for its biological properties in combating various chronic diseases.[18,19] However, the current understanding of UA's effects on colitis is still limited. In this study, we demonstrated that 25 mg/kg of UA offers significant protection against colitis, as evidenced by improvements in weight loss, colon length reduction, DAI scores, and decreased histological scores.

The incidence and severity of IBD are closely associated with Treg/Th17 imbalance.[32] Pathogenic Th17 cells are distinguished by the expression of RORγt, which drives IL-17A production and enhances secretion of pro-inflammatory mediators. This cascade triggers an exaggerated inflammatory response within the gut, promoting the progression of IBD.[33,34] Conversely, Foxp3+ Treg cells function as key immune regulators, suppressing Th17 activity and secreting anti-inflammatory IL-10.[35] Additionally, activation of the Stat3 pathway by IL-6 promotes Th17 cell differentiation through the induction of RORγt expression,[36] while TGF-β facilitates Treg cell differentiation by stimulating Foxp3 transcription.[6] Our investigation demonstrated that UA treatment markedly alleviated colitis-associated inflammation in mice, showing decreased pro-inflammatory cytokines and elevated anti-inflammatory mediators. Additionally, the increased expression of *Foxp3*, *TGF-β*, and *IL-10* mRNA, along with elevated Foxp3 protein levels in the colon of the DSS + UA group compared to the DSS group, suggested enhanced Treg cell differentiation. Conversely, the decreased mRNA expression of *RORγt*, *IL-6*, and *IL-17A*, along with reduced protein levels of RORγt, indicated diminished differentiation of the Th17 cells. Thus, UA intake effectively restored the balance between Treg and Th17 cells in colitis mice, leading to a reduction in the inflammatory response.

Patients with IBD often exhibit significant "dysbiosis" in their gut microbiota.[37] In our study, UA intake alleviated microbiota dysbiosis in colitis mice, as indicated by an increase in the GMHI and a decrease in the MDI. *Clostridium_sens_stricto_1* is a SCFA-producing bacterium that plays an indirect role in the immunomodulatory process.[38] *Dubosiella* has been shown to restore the Treg/Th17 immune balance and reduce mucosal barrier damage by producing SCFAs, particularly propionate.[39] Moreover, propionic acid has been demonstrated to promote Treg cell proliferation and ameliorate the Treg/Th17 differentiation imbalance.[7,40] We found that UA intake markedly enhanced the abundance of *Clostridium_sens_stricto_1* and *Dubosiella*, along with elevated levels of propionic acid. These results suggest that UA may restore the Treg/Th17 immune balance by promoting the growth of SCFA-producing bacteria and increasing propionic acid concentrations. The definitive causal relationship may require further experimental validation.

Escherichia-Shigella is typically highly prevalent in the intestines of IBD patients and has been linked to the disease's pathogenesis.[41,42] Notably, individuals with IBD who are unresponsive to anti-TNF-α therapy commonly exhibit increased levels of *Escherichia-Shigella*,[8] which has been reported as a marker of adverse drug reactions and is associated with a high recurrence rate in IBD.[43] Surprisingly, the UA intake significantly reversed the increase in *Escherichia-Shigella* caused

https://doi.org/10.1021/acs.jafc.5c00220
J. Agric. Food Chem. XXXX, XXX, XXX−XXX

by DSS. Infection by *Escherichia-Shigella* is characterized by its ability to invade the inner epithelial layer, triggering pyroptosis through inflammasome activation. This pathological progression compromises gut epithelial integrity, resulting in enhanced microbial translocation.[44] As a major constituent of *E. coli*'s outer membrane, LPS binds to TLR4 receptors, initiating a cascade that stimulates the expression of NLRP3, promoting GSDMD-mediated pyroptosis and exacerbating IBD.[45−49] Our results showed that UA ameliorated DSS-induced tight junction integrity damage, significantly inhibited *E. coli* translocation, reduced LPS levels, and suppressed the mRNA expression of pyroptosis-related genes in the colon. Furthermore, *E. coli*, LPS, and inflammatory cytokines were significantly correlated with intestinal barrier-related proteins and histological scores. Collectively, these results indicate that UA may reduce DSS-induced colitis by inhibiting *E. coli* proliferation and LPS production, thereby suppressing pyroptosis and alleviating intestinal barrier damage.

In our results, L-histidine was identified as a potential marker for UA to alleviate DSS-induced colitis. Previous studies have established that histidine biosynthesis, facilitated by gut bacteria, provides protection against colitis,[50] and it has been shown to counteract colitis by decreasing pro-inflammatory cytokine production in macrophages.[51] Moreover, we identified a significant negative correlation between the L-histidine levels and *E. coli* abundance. Previous studies reported that L-histidine inhibits *E. coli* proliferation by increasing oxidative DNA damage.[52,53] We speculate that the beneficial effect of UA on colitis may be mediated through histidine and that the protective effect of histidine may be to act as an *E. coli* inhibitor. Our hypothesis was confirmed by *in vitro* experiments, which indicated that histidine significantly suppressed *E. coli* growth and LPS production and ameliorated the elevated levels of inflammatory cytokines and barrier dysfunction. The NLRP3 inflammasome, an intracellular protein complex, is a key mediator of GSDMD-mediated pyroptosis.[54] A range of stimuli, including exogenous pathogenic invasion and endogenous cell injury, induce NLRP3 oligomer formation, and facilitate apoptosis-associated speck-like protein containing a CARD (ASC) and pro-caspase-1 recruitment, leading to caspase-1 activation. Caspase-1 processes pro-IL-1β into its mature form and cleaves GSDMD to release the N-terminal domain of GSDMD (GSDMD-NT). This domain interacts with membrane lipids, forming pores in the cell membrane, which leads to cell swelling, IL-1β release, and eventual membrane rupture.[49] In our study, L-histidine effectively inhibited pyroptosis induced by *E. coli* infection and the subsequent release of inflammatory cytokines. Thus, our results indicate that the gut microbial metabolite L-histidine mediates UA's inhibitory effects on *E. coli* and LPS, thereby reducing pyroptosis and inflammatory cytokine release and ultimately improving intestinal barrier function.

IBD manifests as an inflammatory disease of the intestine and may also have systemic manifestations. Studies have shown that IBD patients may develop an inflammatory phenotype in the liver due to changes in the gut microbiome.[1] Our research indicated that liver injury induced by DSS in mice was likely linked to the translocation of *E. coli* from the gut and the production of LPS. UA has been shown to ameliorate intestinal leakage and attenuate alcoholic liver disease by modulating the gut−liver axis,[27] which aligns with our findings. Moreover, MAPK, Rap1, and Ras signaling pathways may be implicated in the protective mechanisms of UA against liver injury. The MAPK signaling pathway is known to regulate inflammation and is involved in various inflammatory disorder.[55] The small guanosine triphosphatase (GTPase) Rap1, along with its downstream effector Rap1-interacting molecule (RIAM), plays a crucial role in T cell signaling integration and influences numerous functions related to both innate and adaptive immunity.[56] Ras signaling is pivotal for normal physiological cell proliferation, with its dysregulation being linked to tumorigenesis.[57] Furthermore, KDR and HGF may be the main targets of UA to alleviate liver injury. KDR was shown to be an important regulator of angiogenesis in mouse liver cancer cells.[58] HGF, a significant mediator, influences many inflammatory and immune diseases, and its signaling can exacerbate intestinal inflammatory damage.[59] Prior research has demonstrated that knocking down HGF can reverse liver failure induced by sepsis and decrease mortality rates.[60] Therefore, our study suggests that UA may prevent colitis-induced liver inflammatory changes by inhibiting inflammation-related signaling pathways and the expression of *KDR* and *HGF*.

Nevertheless, certain limitations of this study should be recognized. Although we evaluated T-cell differentiation through ELISA, qRT-PCR, and immunohistochemistry, future studies should incorporate flow cytometry for quantitative analysis of T-cell subsets using fresh samples. Further studies are required to directly assess the impacts of gut microbiota and their metabolites, even though we observed the positive effects of UA on colitis and the associated liver damage in mice and investigated the underlying mechanisms. This could include fecal microbiota transplantation and sterile fecal filtrate assessments. Additionally, developing a liver disease model to further explore the hepatoprotective effects of UA warrants future investigation and validation. We acknowledge that definitive causal evidence and the primary mode of UA's action require further experimental validation (e.g., microbiota depletion, adoptive T-cell transfer, and gene knockout mouse experiment).

Our research clarifies the mechanisms by which UA exerts beneficial effects on colitis and sheds light on its role in alleviating liver injury associated with this condition. Specifically, UA decreased the levels of inflammatory mediators by restoring the Treg/Th17 cells balance, likely linked to the abundance of SCFA-producing bacteria and increased levels of propionic acid. UA inhibits the proliferation of *E. coli* and reduces LPS levels through the microbial metabolite L-histidine, thereby strengthening intestinal barrier function and inhibiting pyroptosis. Furthermore, UA may prevent colitis-induced liver injury by inhibiting inflammation-related signaling pathways, including the MAPK, Rap1, and Ras signaling pathways, as well as by modulating the expression of key proteins, such as *KDR* and *HGF*. Our findings offer important insights for developing strategies to manage IBD, and the potential use of UA as a functional food component could lead to innovative dietary interventions aimed at promoting intestinal health.

■ ASSOCIATED CONTENT

Data Availability Statement

The data that support the study findings are available upon request.

Supporting Information

The Supporting Information is available free of charge at https://pubs.acs.org/doi/10.1021/acs.jafc.5c00220.

https://doi.org/10.1021/acs.jafc.5c00220
J. Agric. Food Chem. XXXX, XXX, XXX−XXX

Histopathology; Quantitative reverse transcription-polymerase chain reaction (qRT-PCR); Immunohistochemistry (IHC); Immunofluorescence (IF); Determination of SCFAs; Bacterial translocation; Western blot assay; Gene-specific primer sequences used for gene transcription analyses; Antibodies used in this study for Western blot; Effect of UA treatment on percent survival in colitis mice; Negative control staining images of immunohistochemical staining (without primary antibody); Effect of UA treatment on intestinal microbial composition in colitis mice; Comparison of differences in the relative abundance of bacteria at the genus level; Comparison of differences in the relative abundance of bacteria at the species level; Heatmap of Spearman's correlations between differential microbiota and metabolites; Analysis of differences in transcriptome data of each group; Verification of the expression levels of 10 mRNAs using qRT-PCR; WGCNA analysis of liver transcriptome in mice (PDF)

AUTHOR INFORMATION

Corresponding Authors

Shuaijuan Han − *College of Animal Science and Technology, Hebei Agricultural University, Baoding 071000, China*; Email: hansjuan@163.com

Baojiang Chen − *College of Animal Science and Technology, Hebei Agricultural University, Baoding 071000, China*; orcid.org/0000-0002-7193-6055; Email: 199051@hebau.edu.cn

Authors

Man Zhao − *College of Animal Science and Technology, Hebei Agricultural University, Baoding 071000, China*

Mengqi Liu − *College of Animal Science and Technology, Henan Agricultural University, Zhengzhou 450002, China*

Fengyang Wu − *College of Animal Science and Technology, Hebei Agricultural University, Baoding 071000, China*

Chong Li − *College of Animal Science and Technology, Hebei Agricultural University, Baoding 071000, China*

Shudong Liu − *College of Animal Science and Technology, Hebei Agricultural University, Baoding 071000, China*

Xinyu Yang − *College of Animal Science and Technology, Hebei Agricultural University, Baoding 071000, China*

Zhonghua Wei − *Hebei Institute of Animal Husbandry and Veterinary Medicine, Baoding 071000, China*

Complete contact information is available at: https://pubs.acs.org/10.1021/acs.jafc.5c00220

Author Contributions

M.Z.: conceptualization, data curation, formal analysis, funding acquisition, methodology, visualization, writing − original draft. M.L.: data curation, methodology, writing − original draft. F.W.: data curation, formal analysis, writing − original draft. C.L.: validation, methodology. S.L.: validation, methodology. X.Y.: validation, methodology. Z.W.: validation, methodology. B.C.: conceptualization, funding acquisition, project administration, writing − review and editing. S.H.: funding acquisition, validation, methodology, project administration, writing − review and editing.

Author Contributions

‖M.Z., M.L., and F.W. contributed equally to this work

Funding

This study received financial support from the National Key Research and Development Program of China (2024YFD1300805), the Modern Agriculture Industry Technology System of Rabbit, China (CARS-43-B-2), the Innovation Team of Hebei Special Livestock Breeding Industry Technology System (HBCT2024280204), and the Postgraduate Innovation Funding Project of Hebei Province (CXZZBS2024075).

Notes

The authors declare no competing financial interest.

REFERENCES

(1) Rohwer, N.; Jelleschitz, J.; Höhn, A.; Weber, D.; Kühl, A. A.; Wang, C.; Ohno, R. I.; Kampschulte, N.; Pietzner, A.; Schebb, N. H.; Weylandt, K. H.; Grune, T. Prevention of colitis-induced liver oxidative stress and inflammation in a transgenic mouse model with increased omega-3 polyunsaturated fatty acids. *Redox biology* **2023**, *64*, No. 102803.

(2) Ng, S. C.; Shi, H. Y.; Hamidi, N.; Underwood, F. E.; Tang, W.; Benchimol, E. I.; Panaccione, R.; Ghosh, S.; Wu, J. C. Y.; Chan, F. K. L.; Sung, J. J. Y.; Kaplan, G. G. Worldwide incidence and prevalence of inflammatory bowel disease in the 21st century: a systematic review of population-based studies. *Lancet (London, England)* **2017**, *390* (10114), 2769−2778.

(3) Wang, Y.; Li, Q.; Zhang, J.; Liu, P.; Zheng, H.; Chen, L.; Wang, Z.; Tan, C.; Zhang, M.; Zhang, H.; Miao, W.; Wang, Y.; Xuan, X.; Yi, G.; Wang, P. Ring1a protects against colitis through regulating mucosal immune system and colonic microbial ecology. *Gut microbes* **2023**, *15* (2), No. 2251646.

(4) Dong, L.; Xie, J.; Wang, Y.; Jiang, H.; Chen, K.; Li, D.; Wang, J.; Liu, Y.; He, J.; Zhou, J.; Zhang, L.; Lu, X.; Zou, X.; Wang, X. Y.; Wang, Q.; Chen, Z.; Zuo, D. Mannose ameliorates experimental colitis by protecting intestinal barrier integrity. *Nat. Commun.* **2022**, *13*, 4804.

(5) Liu, Y. J.; Tang, B.; Wang, F. C.; Tang, L.; Lei, Y. Y.; Luo, Y.; Huang, S. J.; Yang, M.; Wu, L. Y.; Wang, W.; Liu, S.; Yang, S. M.; Zhao, X. Y. Parthenolide ameliorates colon inflammation through regulating Treg/Th17 balance in a gut microbiota-dependent manner. *Theranostics* **2020**, *10* (12), 5225−5241.

(6) Wang, J.; Zhao, X.; Wan, Y. Y. Intricacies of TGF-β signaling in Treg and Th17 cell biology. *Cellular & molecular immunology* **2023**, *20* (9), 1002−1022.

(7) Du, H. X.; Yue, S. Y.; Niu, D.; Liu, C.; Zhang, L. G.; Chen, J.; Chen, Y.; Guan, Y.; Hua, X. L.; Li, C.; Chen, X. G.; Zhang, L.; Liang, C. Z. Gut Microflora Modulates Th17/Treg Cell Differentiation in Experimental Autoimmune Prostatitis via the Short-Chain Fatty Acid Propionate. *Frontiers in immunology* **2022**, *13*, No. 915218.

(8) Wang, C.; Gu, Y.; Chu, Q.; Wang, X.; Ding, Y.; Qin, X.; Liu, T.; Wang, S.; Liu, X.; Wang, B.; Cao, H. Gut microbiota and metabolites as predictors of biologics response in inflammatory bowel disease: A comprehensive systematic review. *Microbiological research* **2024**, *282*, No. 127660.

(9) Sun, B.; Wang, Y.; Bai, J.; Li, X.; Ma, L.; Man, S. Litchi Procyanidins Ameliorate DSS-Induced Colitis through Gut Microbiota-Dependent Regulation of Treg/Th17 Balance. *Journal of agricultural and food chemistry* **2024**, *72* (44), 24823−24832.

(10) Jia, D. J.; Wang, Q. W.; Hu, Y. Y.; He, J. M.; Ge, Q. W.; Qi, Y. D.; Chen, L. Y.; Zhang, Y.; Fan, L. N.; Lin, Y. F.; Sun, Y.; Jiang, Y.; Wang, L.; Fang, Y. F.; He, H. Q.; Pi, X. E.; Liu, W.; Chen, S. J.; Wang, L. J. Lactobacillus johnsonii alleviates colitis by TLR1/2-STAT3 mediated CD206(+) macrophages(IL-10) activation. *Gut microbes* **2022**, *14* (1), No. 2145843.

(11) Yan, Y.; Lei, Y.; Qu, Y.; Fan, Z.; Zhang, T.; Xu, Y.; Du, Q.; Brugger, D.; Chen, Y.; Zhang, K.; Zhang, E. Bacteroides uniformis-induced perturbations in colonic microbiota and bile acid levels inhibit TH17 differentiation and ameliorate colitis developments. *NPJ. biofilms and microbiomes* **2023**, *9*, 56.

(12) Han, M.; Liang, J.; Hou, M.; Liu, Y.; Li, H.; Gao, Z. Bifidobacterium bifidum Ameliorates DSS-Induced Colitis in Mice by

Regulating Microbial Metabolome and Targeting Gut Microbiota. *Journal of agricultural and food chemistry* **2024**, *72*, 13593.
(13) Li, M.; Han, X.; Sun, L.; Liu, X.; Zhang, W.; Hao, J. Indole-3-acetic acid alleviates DSS-induced colitis by promoting the production of R-equol from Bifidobacterium pseudolongum. *Gut microbes* **2024**, *16* (1), No. 2329147.
(14) Navarro, P.; Gutiérrez-Ramírez, L.; Tejera-Muñoz, A.; Arias, Á.; Lucendo, A. J. Systematic Review and Meta-Analysis: Prevalence of Non-Alcoholic Fatty Liver Disease and Liver Fibrosis in Patients with Inflammatory Bowel Disease. *Nutrients* **2023**, *15* (21), 4507.
(15) Tripathi, A.; Debelius, J.; Brenner, D. A.; Karin, M.; Loomba, R.; Schnabl, B.; Knight, R. The gut-liver axis and the intersection with the microbiome. *Nature reviews. Gastroenterology & hepatology* **2018**, *15* (7), 397−411.
(16) van Munster, K. N.; Bergquist, A.; Ponsioen, C. Y. Inflammatory bowel disease and primary sclerosing cholangitis: One disease or two? *Journal of hepatology* **2024**, *80* (1), 155−168.
(17) Chen, B.; Luo, J.; Han, Y.; Du, H.; Liu, J.; He, W.; Zhu, J.; Xiao, J.; Wang, J.; Cao, Y.; Xiao, H.; Song, M. Dietary Tangeretin Alleviated Dextran Sulfate Sodium-Induced Colitis in Mice via Inhibiting Inflammatory Response, Restoring Intestinal Barrier Function, and Modulating Gut Microbiota. *Journal of agricultural and food chemistry* **2021**, *69* (27), 7663−7674.
(18) Zhao, M.; Wu, F.; Tang, Z.; Yang, X.; Liu, Y.; Wang, F.; Chen, B. Anti-inflammatory and antioxidant activity of ursolic acid: a systematic review and meta-analysis. *Frontiers in pharmacology* **2023**, *14*, No. 1256946.
(19) Jang, S. E.; Jeong, J. J.; Hyam, S. R.; Han, M. J.; Kim, D. H. Ursolic acid isolated from the seed of Cornus officinalis ameliorates colitis in mice by inhibiting the binding of lipopolysaccharide to Toll-like receptor 4 on macrophages. *Journal of agricultural and food chemistry* **2014**, *62* (40), 9711−21.
(20) Zhao, H.; Tang, S.; Tao, Q.; Ming, T.; Lei, J.; Liang, Y.; Peng, Y.; Wang, M.; Liu, M.; Yang, H.; Ren, S.; Xu, H. Ursolic Acid Suppresses Colorectal Cancer by Down-Regulation of Wnt/β-Catenin Signaling Pathway Activity. *Journal of agricultural and food chemistry* **2023**, *71* (9), 3981−3993.
(21) Zhang, C.; Wang, M.; Liu, H.; Jiang, X.; Chen, X.; Liu, T.; Yin, Q.; Wang, Y.; Deng, L.; Yao, J.; Wu, S. Multi-omics reveals that the host-microbiome metabolism crosstalk of differential rumen bacterial enterotypes can regulate the milk protein synthesis of dairy cows. *Journal of animal science and biotechnology* **2023**, *14*, 63.
(22) Zheng, Y.; Zhao, L.; Xiong, Z.; Huang, C.; Yong, Q.; Fang, D.; Fu, Y.; Gu, S.; Chen, C.; Li, J.; Zhu, Y.; Liu, J.; Liu, F.; Li, Y. Ursolic acid targets secreted phosphoprotein 1 to regulate Th17 cells against metabolic dysfunction-associated steatotic liver disease. *Clinical and molecular hepatology* **2024**, *30* (3), 449−467.
(23) Nie, Y.; Liu, Q.; Zhang, W.; Wan, Y.; Huang, C.; Zhu, X. Ursolic acid reverses liver fibrosis by inhibiting NOX4/NLRP3 inflammasome pathways and bacterial dysbiosis. *Gut microbes* **2021**, *13* (1), No. 1972746.
(24) Sheng, Q.; Li, F.; Chen, G.; Li, J.; Li, J.; Wang, Y.; Lu, Y.; Li, Q.; Li, M.; Chai, K. Ursolic Acid Regulates Intestinal Microbiota and Inflammatory Cell Infiltration to Prevent Ulcerative Colitis. *Journal of immunology research* **2021**, *2021*, No. 6679316.
(25) Hou, M.; Shi, J.; Lin, C.; Zhu, L.; Bian, Z. Ultrasound-assisted extraction of triterpenoids from Chaenomeles speciosa leaves: Process optimization, adsorptive enrichment, chemical profiling, and protection against ulcerative colitis. *Ultrasonics sonochemistry* **2024**, *111*, No. 107136.
(26) Wang, T.; Su, X.; Peng, J.; Tan, X.; Yang, G.; Zhang, T.; Chen, F.; Wang, C.; Ma, K. Deciphering the pharmacological mechanisms of Fraxini Cortex for ulcerative colitis treatment based on network pharmacology and in vivo studies. *BMC complementary medicine and therapies* **2023**, *23*, 152.
(27) Yan, X.; Ren, X.; Liu, X.; Wang, Y.; Ma, J.; Song, R.; Wang, X.; Dong, Y.; Fan, Q.; Wei, J.; Yu, A.; She, G. Dietary Ursolic Acid Prevents Alcohol-Induced Liver Injury via Gut-Liver Axis Homeostasis Modulation: The Key Role of Microbiome Manipulation. *Journal of agricultural and food chemistry* **2021**, *69* (25), 7074−7083.
(28) Zhao, M.; Cui, Y.; Wang, F.; Wu, F.; Li, C.; Liu, S.; Chen, B. Ursolic Acid Regulates Immune Balance, Modulates Gut Microbial Metabolism, and Improves Liver Health in Mice. *International journal of molecular sciences* **2024**, *25* (19), 10623.
(29) Gupta, V. K.; Kim, M.; Bakshi, U.; Cunningham, K. Y.; Davis, J. M., 3rd; Lazaridis, K. N.; Nelson, H.; Chia, N.; Sung, J. A predictive index for health status using species-level gut microbiome profiling. *Nat. Commun.* **2020**, *11* (1), 4635.
(30) Xu, R.; Wu, B.; Liang, J.; He, F.; Gu, W.; Li, K.; Luo, Y.; Chen, J.; Gao, Y.; Wu, Z.; Wang, Y.; Zhou, W.; Wang, M. Altered gut microbiota and mucosal immunity in patients with schizophrenia. *Brain, behavior, and immunity* **2020**, *85*, 120−127.
(31) Li, Q.; Chao, T.; Wang, Y.; Xuan, R.; Guo, Y.; He, P.; Zhang, L.; Wang, J. Transcriptome analysis reveals miRNA expression profiles in hypothalamus tissues during the sexual development of Jining grey goats. *BMC genomics* **2024**, *25*, 832.
(32) Li, M.; Guo, W.; Dong, Y.; Wang, W.; Tian, C.; Zhang, Z.; Yu, T.; Zhou, H.; Gui, Y.; Xue, K.; Li, J.; Jiang, F.; Sarapultsev, A.; Wang, H.; Zhang, G.; Luo, S.; Fan, H.; Hu, D. Beneficial Effects of Celastrol on Immune Balance by Modulating Gut Microbiota in Experimental Ulcerative Colitis Mice. *Genomics, proteomics & bioinformatics* **2022**, *20* (2), 288−303.
(33) Britton, G. J.; Contijoch, E. J.; Mogno, I.; Vennaro, O. H.; Llewellyn, S. R.; Ng, R.; Li, Z.; Mortha, A.; Merad, M.; Das, A.; Gevers, D.; McGovern, D. P. B.; Singh, N.; Braun, J.; Jacobs, J. P.; Clemente, J. C.; Grinspan, A.; Sands, B. E.; Colombel, J. F.; Dubinsky, M. C.; Faith, J. J. Microbiotas from Humans with Inflammatory Bowel Disease Alter the Balance of Gut Th17 and RORγt(+) Regulatory T Cells and Exacerbate Colitis in Mice. *Immunity* **2019**, *50* (1), 212.
(34) Geremia, A.; Biancheri, P.; Allan, P.; Corazza, G. R.; Di Sabatino, A. Innate and adaptive immunity in inflammatory bowel disease. *Autoimmunity reviews* **2014**, *13* (1), 3−10.
(35) Clough, J. N.; Omer, O. S.; Tasker, S.; Lord, G. M.; Irving, P. M. Regulatory T-cell therapy in Crohn's disease: challenges and advances. *Gut* **2020**, *69* (5), 942−952.
(36) Wei, L.; Laurence, A.; O'Shea, J. J. New insights into the roles of Stat5a/b and Stat3 in T cell development and differentiation. *Seminars in cell & developmental biology* **2008**, *19* (4), 394−400.
(37) Yi, L.; Han, Y.; Shen, P.; Du, H.; Guo, X.; Zhou, Z.; Xiao, H. Dietary Porphyra tenera ameliorated dextran sodium sulfate-induced colitis in mice via modulating gut microbiota dysbiosis. *Food chemistry* **2024**, *461*, No. 140832.
(38) Chen, Y. Y.; Chen, S. Y.; Chang, H. Y.; Liu, Y. C.; Chuang, B. F.; Yen, G. C. Phyllanthus emblica L. polysaccharides ameliorate colitis via microbiota modulation and dual inhibition of the RAGE/NF-κB and MAPKs signaling pathways in rats. *Int. J. Biol. Macromol.* **2024**, *258*, No. 129043.
(39) Zhang, Y.; Tu, S.; Ji, X.; Wu, J.; Meng, J.; Gao, J.; Shao, X.; Shi, S.; Wang, G.; Qiu, J.; Zhang, Z.; Hua, C.; Zhang, Z.; Chen, S.; Zhang, L.; Zhu, S. J. Dubosiella newyorkensis modulates immune tolerance in colitis via the L-lysine-activated AhR-IDO1-Kyn pathway. *Nat. Commun.* **2024**, *15*, 1333.
(40) Duscha, A.; Gisevius, B.; Hirschberg, S.; Yissachar, N.; Stangl, G. I.; Dawin, E.; Bader, V.; Haase, S.; Kaisler, J.; David, C.; Schneider, R.; Troisi, R.; Zent, D.; Hegelmaier, T.; Dokalis, N.; Gerstein, S.; Del Mare-Roumani, S.; Amidror, S.; Staszewski, O.; Poschmann, G.; Stühler, K.; Hirche, F.; Balogh, A.; Kempa, S.; Träger, P.; Zaiss, M. M.; Holm, J. B.; Massa, M. G.; Nielsen, H. B.; Faissner, A.; Lukas, C.; Gatermann, S. G.; Scholz, M.; Przuntek, H.; Prinz, M.; Forslund, S. K.; Winklhofer, K. F.; Müller, D. N.; Linker, R. A.; Gold, R.; Haghikia, A. Propionic Acid Shapes the Multiple Sclerosis Disease Course by an Immunomodulatory Mechanism. *Cell* **2020**, *180* (6), 1067.
(41) Yang, H.; Mirsepasi-Lauridsen, H. C.; Struve, C.; Allaire, J. M.; Sivignon, A.; Vogl, W.; Bosman, E. S.; Ma, C.; Fotovati, A.; Reid, G. S.; Li, X.; Petersen, A. M.; Gouin, S. G.; Barnich, N.; Jacobson, K.; Yu, H. B.; Krogfelt, K. A.; Vallance, B. A. Ulcerative Colitis-associated E. coli

https://doi.org/10.1021/acs.jafc.5c00220
J. Agric. Food Chem. XXXX, XXX, XXX−XXX

pathobionts potentiate colitis in susceptible hosts. *Gut microbes* **2020**, *12* (1), No. 1847976.
(42) Harnack, C.; Berger, H.; Liu, L.; Mollenkopf, H. J.; Strowig, T.; Sigal, M. Short-term mucosal disruption enables colibactin-producing E. coli to cause long-term perturbation of colonic homeostasis. *Gut microbes* **2023**, *15* (1), No. 2233689.
(43) Radhakrishnan, S. T.; Alexander, J. L.; Mullish, B. H.; Gallagher, K. I.; Powell, N.; Hicks, L. C.; Hart, A. L.; Li, J. V.; Marchesi, J. R.; Williams, H. R. T. Systematic review: the association between the gut microbiota and medical therapies in inflammatory bowel disease. *Alimentary pharmacology & therapeutics* **2022**, *55* (1), 26−48.
(44) Taebnia, N.; Römling, U.; Lauschke, V. M. In vitro and ex vivo modeling of enteric bacterial infections. *Gut microbes* **2023**, *15* (1), No. 2158034.
(45) Zhao, C.; Hu, X.; Bao, L.; Wu, K.; Zhao, Y.; Xiang, K.; Li, S.; Wang, Y.; Qiu, M.; Feng, L.; Meng, X.; Zhang, N.; Fu, Y. Gut dysbiosis induces the development of mastitis through a reduction in host anti-inflammatory enzyme activity by endotoxemia. *Microbiome* **2022**, *10*, 205.
(46) Chen, X.; Liu, G.; Yuan, Y.; Wu, G.; Wang, S.; Yuan, L. NEK7 interacts with NLRP3 to modulate the pyroptosis in inflammatory bowel disease via NF-κB signaling. *Cell death & disease* **2019**, *10* (12), 906.
(47) Tong, L.; Hao, H.; Zhang, Z.; Lv, Y.; Liang, X.; Liu, Q.; Liu, T.; Gong, P.; Zhang, L.; Cao, F.; Pastorin, G.; Lee, C. N.; Chen, X.; Wang, J. W.; Yi, H. Milk-derived extracellular vesicles alleviate ulcerative colitis by regulating the gut immunity and reshaping the gut microbiota. *Theranostics* **2021**, *11* (17), 8570−8586.
(48) Larabi, A.; Barnich, N.; Nguyen, H. T. T. New insights into the interplay between autophagy, gut microbiota and inflammatory responses in IBD. *Autophagy* **2020**, *16* (1), 38−51.
(49) Yu, P.; Zhang, X.; Liu, N.; Tang, L.; Peng, C.; Chen, X. Pyroptosis: mechanisms and diseases. *Signal transduction and targeted therapy* **2021**, *6*, 128.
(50) Zeng, W.; Wu, J.; Xie, H.; Xu, H.; Liang, D.; He, Q.; Yang, X.; Liu, C.; Gong, J.; Zhang, Q.; Luo, Z.; Chen, Y.; He, Z.; Lan, P. Enteral nutrition promotes the remission of colitis by gut bacteria-mediated histidine biosynthesis. *EBioMedicine* **2024**, *100*, No. 104959.
(51) Andou, A.; Hisamatsu, T.; Okamoto, S.; Chinen, H.; Kamada, N.; Kobayashi, T.; Hashimoto, M.; Okutsu, T.; Shimbo, K.; Takeda, T.; Matsumoto, H.; Sato, A.; Ohtsu, H.; Suzuki, M.; Hibi, T. Dietary histidine ameliorates murine colitis by inhibition of proinflammatory cytokine production from macrophages. *Gastroenterology* **2009**, *136* (2), 564.
(52) Nagao, T.; Nakayama-Imaohji, H.; Elahi, M.; Tada, A.; Toyonaga, E.; Yamasaki, H.; Okazaki, K.; Miyoshi, H.; Tsuchiya, K.; Kuwahara, T. L-histidine augments the oxidative damage against Gram-negative bacteria by hydrogen peroxide. *International journal of molecular medicine* **2018**, *41* (5), 2847−2854.
(53) Haja Hameed, A. S.; Louis, G.; Karthikeyan, C.; Thajuddin, N.; Ravi, G. Impact of l-Arginine and l-Histidine on the structural, optical and antibacterial properties of Mg doped ZnO nanoparticles tested against extended-spectrum beta-lactamases (ESBLs) producing Escherichia coli. *Spectrochimica acta. Part A, Molecular and biomolecular spectroscopy* **2019**, *211*, 373−382.
(54) Coll, R. C.; Schroder, K.; Pelegrín, P. NLRP3 and pyroptosis blockers for treating inflammatory diseases. *Trends in pharmacological sciences* **2022**, *43* (8), 653−668.
(55) Brenner, C.; Galluzzi, L.; Kepp, O.; Kroemer, G. Decoding cell death signals in liver inflammation. *Journal of hepatology* **2013**, *59* (3), 583−94.
(56) Patsoukis, N.; Bardhan, K.; Weaver, J. D.; Sari, D.; Torres-Gomez, A.; Li, L.; Strauss, L.; Lafuente, E. M.; Boussiotis, V. A. The adaptor molecule RIAM integrates signaling events critical for integrin-mediated control of immune function and cancer progression. *Science Signaling* **2017**, *10*, eaam8298.
(57) Punekar, S. R.; Velcheti, V.; Neel, B. G.; Wong, K. K. The current state of the art and future trends in RAS-targeted cancer therapies. *Nature reviews. Clinical oncology* **2022**, *19* (10), 637−655.
(58) Yoshiji, H.; Kuriyama, S.; Hicklin, D. J.; Huber, J.; Yoshii, J.; Miyamoto, Y.; Kawata, M.; Ikenaka, Y.; Nakatani, T.; Tsujinoue, H.; Fukui, H. KDR/Flk-1 is a major regulator of vascular endothelial growth factor-induced tumor development and angiogenesis in murine hepatocellular carcinoma cells. *Hepatology (Baltimore, Md.)* **1999**, *30* (5), 1179−86.
(59) Stakenborg, M.; Verstockt, B.; Meroni, E.; Goverse, G.; De Simone, V.; Verstockt, S.; Di Matteo, M.; Czarnewski, P.; Villablanca, E. J.; Ferrante, M.; Boeckxstaens, G. E.; Mazzone, M.; Vermeire, S.; Matteoli, G. Neutrophilic HGF-MET Signalling Exacerbates Intestinal Inflammation. *Journal of Crohn's colitis* **2020**, *14* (12), 1748−1758.
(60) Elias, G.; Schonfeld, M.; Saleh, S.; Parrish, M.; Barmanova, M.; Weinman, S. A.; Tikhanovich, I. Sepsis-induced endothelial dysfunction drives acute-on-chronic liver failure through Angiopoietin-2-HGF-C/EBPβ pathway. *Hepatology (Baltimore, Md.)* **2023**, *78* (3), 803−819.

https://doi.org/10.1021/acs.jafc.5c00220
J. Agric. Food Chem. XXXX, XXX, XXX−XXX